Published in final edited form as:

Biochemistry. 2017 July 18; 56(28): 3523–3530. doi:10.1021/acs.biochem.7b00100.

HDX MS reveals calcium binding properties and allosteric regulation of downstream regulatory element antagonist modulator (DREAM)

Jun Zhang[1,†,‼], **Jing Li**[1,‡,‼], **Theodore A. Craig**[2,*], and **Michael L. Gross**[1,*]

[1]Department of Chemistry, Washington University in St. Louis, St. Louis, MO 63130, USA

[2]Division of Nephrology and Hypertension, Department of Medicine, Mayo Clinic, Rochester, MN 55905, USA

Abstract

Downstream regulatory element antagonist modulator (DREAM) is an EF-hand Ca^{2+}-binding protein that also binds to specific DNA sequence, downstream regulatory elements (DRE), and thereby regulates transcription in a calcium-dependent fashion. DREAM binds to DRE in the absence of Ca^{2+}, but detaches from DRE under Ca^{2+} stimulation, allowing gene expression. The Ca^{2+}-binding properties of DREAM and the consequences of the binding on protein structure are key to understanding the function of DREAM. Here we describe the application of hydrogen deuterium exchange mass spectrometry (HDX-MS) and site-directed mutagenesis to investigate the Ca^{2+} binding properties and the subsequent conformational changes of full length DREAM. We demonstrate that all EF-hands undergo large conformation changes upon calcium binding even though EF-1 hand is not capable of binding to Ca^{2+}. Moreover, EF-2 is a weaker affinity site compared to EF-3 and 4 hands. Comparison of HDX profiles between WT DREAM and two EF-1 mutated constructs illustrate that the conformational changes in EF-1 hand are induced by long-range structural interactions. HDX analyses also reveal a conformational change in an N-terminal leucine-charged residue-rich domain (LCD) remote from Ca^{2+} binding EF-hands. This LCD domain is responsible for the direct interaction between DREAM and cAMP response element-binding protein (CREB) and regulates the recruitment of coactivator, CREB-binding protein (CBP). These long-range interactions strongly suggest how conformational changes transmit the Ca^{2+} signal to CREB-mediated gene transcription.

Graphical Abstract

[*]Address correspondence to: Michael L. Gross, Department of Chemistry, Washington University in St. Louis, St. Louis, MO 63130, USA, Phone: 314-935-4814, mgross@wustl.edu; Rajiv Kumar, Division of Nephrology and Hypertension, Department of Medicine, Mayo Clinic, Rochester, MN USA rkumar@mayo.edu.

[†]Current address: Jun Zhang, Pre-pivotal Drug Product Technology, Amgen Inc., Thousand Oaks, CA 91320

[‡]Current address: Jing Li, Structural Biology and Biophysics, Takeda Pharmaceuticals USA, San Diego, CA 92121

[‼]Contributed equally to the article; co-first authors.

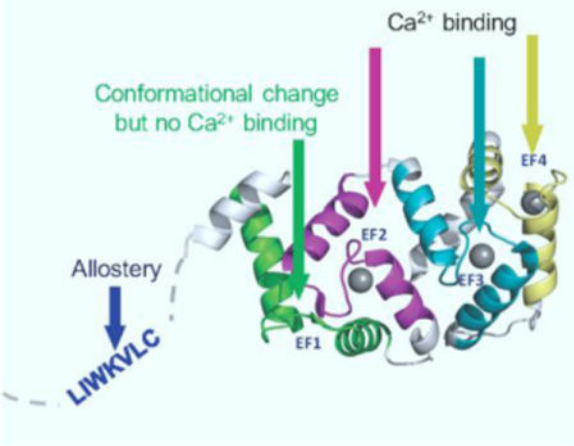

Introduction

DREAM (downstream regulatory element antagonist modulator) was initially discovered as the first calcium-binding protein that functions as a transcriptional repressor of prodynorphin and *c-fos* genes[1]. DREAM serves as a transcriptional repressor of prodynorphic and *c-fos* gene expression by binding to the downstream regulatory elements (DRE) in the promoter of its target genes[1]. So far, DREAM is the only known Ca^{2+}-binding protein that binds to specific DRE sequences and directly regulates transcription in a calcium-dependent fashion. DREAM can only bind to DRE sequences in the Ca^{2+}-free state, whereas Ca^{2+} binding to DREAM induces conformational changes that abolish its ability to bind to DRE[1–3].

DREAM, a 256 amino-acid protein, contains four Ca^{2+}-binding motifs (EF-hands) arranged in a globular structure. Each EF hand is, as usual, a helix-loop-helix motif containing a short loop where calcium binds and links two alpha helices[4]. DREAM may exist as a small oligomer when interacting with the DREs of target genes[2, 5], and the interaction is Ca^{2+}-binding dependent. To understand better how calcium binding regulates the structure and function of DREAM, considerable effort has been devoted to gain structural insights into the calcium-binding properties and the induced conformational changes.

The structure of the EF-1 loop in DREAM is distorted from a favorable Ca^{2+}-binding geometry by the presence of CPXG (Cys 104 and Pro 105), similar to that seen in other structure of the neuronal calcium sensor (NCS) proteins[2]. The presence of Cys 104 at position 3, which usually has an oxygen ligand, and the shorter length (Table 1) indicate this loop is “non-canonical”[6]. The CPXG sequence apparently prevents the binding of Ca^{2+} to the first EF-hand. The second, third and fourth, EF-hands are highly conserved with the EF-hand consensus[1]. EF-hands 2,3,4 can be viewed as “canonical EF loops”[6] (Table 1).

An NMR structure of the N-terminal truncated DREAM with bound Ca^{2+} is available, and structural analyses suggest Ca^{2+}-induced protein dimerization may serve to block sterically its ability to bind to DRE and thereby depresses transcription[7]. To date, there is little structural information about full length DREAM (FL-DREAM). The N-terminus (residues 1–65) of FL-DREAM may not be functionally important as the truncated constructs are still

fully active in some biological assays[7]; however, this region contains a leucine-charged domain at position 47, which does govern the interactions between DREAM and CREB and thereby regulating the transcription of the downstream genes[20, 21].

Hydrogen/deuterium exchange mass spectrometry (HDX-MS) has emerged as a powerful means to characterize protein structure and dynamics. HDX-MS reports on the hydrogen bonding and solvent accessibility of the protein backbone amide hydrogens[8, 9] and is sensitive to protein structural changes caused by different perturbations (e.g., DNA binding[10], protein-protein interactions[11], changes in pH[12], and aggregation[13]). In this work, we used HDX-MS to probe the impact of Ca^{2+} binding on the protein structure and dynamics of an intact DREAM. These investigations represent, to our knowledge, the first detailed structural analyses of a full-length DREAM. Our HDX analyses demonstrate that Ca^{2+} binds at EF-hand 2, 3, and 4 accompanied by a remote conformation change in the first EF-hand. More importantly, a leucine-charged domain (AA 46–52), remote of the EF hands, shows significant protection with the addition of calcium. This region is critical for the interaction with cAMP response element-binding protein (CREB), thereby mediating transactivation at CRE site as a proposed allosteric change.

Experimental Procedures

Materials

All chemicals, proteases and solvents were purchased from Sigma Aldrich (St. Louis, MO) unless otherwise stated. Deuterium oxide was purchased from Cambridge Isotope Laboratories Inc. (Andover, MA). The POROS 20 AL beads used to pack immobilized porcine pepsin columns were purchased from Applied Biosystems (Grand Island, NY).

Synthesis of Wild-Type, E111Q/D112N and E103A/D110A DREAM

DREAM wild type protein was expressed as an N-terminal glutathione S-transferase (GST) fusion protein containing an intervening PreScission protease cleavage site, in pGEX-6P-1 vector/*Escherichia coli* BL21 host (GE Healthcare, Pittsburgh, PA) (as described previously)[1–3].

The fusion protein was proteolytically cleaved leaving the full length DREAM with five residues (GPLGS) as an N-terminal addition to the DREAM sequence. DREAM mutants were synthesized utilizing the full-length human DREAM-KChIP3 cDNA templates in pGEX-6P-1 as a GST fusion for mutant E111Q/D112N DREAM, or in pET28a(+) with a 6XHis tag for mutant E103A/D110A DREAM using the QuikChange Lightning Multi-Site Mutagenesis Kit (Agilent Technologies, Santa Clara, CA) according to the manufacturer's instructions[5, 14, 15]. Appropriate primers with mutations were synthesized. Single-stranded mutant DNA was amplified in XL10-Gold ultra-competent *Escherichia coli* cells. The mutant protein, E111Q/D112N DREAM was expressed in *E. coli* Rosetta2 (*DE3*) cells (EMD-Millipore, Billerica, MA) grown in the presence of 2X YT medium containing ampicillin (100 μg/mL) and chloramphenicol (50 μg/mL). The E103A/D110A DREAM protein was expressed in *E. coli* Rosetta2 (*DE3*) cells grown in the presence 2X YT medium containing kanamycin (40 μg/mL) and chloramphenicol (50 μg/mL). *E. coli* cells expressing

the appropriate protein, following induction with isopropyl β-D-thiogalactopyranoside (IPTG), were lysed in a Bead Beater apparatus (Biospec Products, Bartlesville, OK), and fusion proteins were purified on Glutathione Sepharose (GE Healthcare) (E111Q/D112N DREAM) or Ni Sepharose 6 FF (GE Healthcare) (E103A/D110A DREAM) affinity columns according to manufacturer recommendations. Mutant DREAM proteins were cleaved at the PreScission protease site yielding E111Q/D112N DREAM with five additional residues (GPLGS) at the N-terminus, and the E103A/D110A DREAM with two additional residues (GP) at the N-terminus.

Hydrogen Deuterium Exchange Mass Spectrometry

The HDX reactions for the wild type FL-DREAM were performed at three conditions: apo (2 mM EGTA), holo (low Ca^{2+}, 100 μM), and holo (high Ca^{2+}, 5 mM), respectively. Apo and holo (low Ca^{2+}) DREAM samples were prepared by equilibrating the wild-type DREAM (50 μM) protein in the presence of 2 mM EGTA (*apo* protein) or 2 mM $CaCl_2$ (holo protein) for at least 2 h at 4 ºC. The HDX was initiated by diluting 1 μL of protein (50 μM) 20-fold with D_2O buffer (50 mM Tris, 150 mM KCl, 1 mM DTT, pH 7.3) or H_2O buffer for samples measured for no deuterium control. It should be noted that the active concentration of EGTA and Ca^{2+} are both 100 μM during the time course of the HDX labeling. When the protein was incubated at a high calcium concentration (5 mM), the protein was considered to be saturated with Ca^{2+}, and the HDX reaction was employed by diluting 20-fold with the same D_2O buffer but containing 5 mM $CaCl_2$ to maintain Ca^{2+}-saturation of DREAM after dilution. HDX for EF-1 hand mutants was only studied at a calcium concentration at 100 μM. At different exchange time intervals, (10, 30, 60, 360, 900, 3600, and 14400 s), the labeling reaction was quenched by adjusting the pH to 2.5 with 30 μL of ice-cold quench buffer (3 M urea, 1% trifluoroacetic acid, H_2O).

For intact HDX analysis, the protein mixture was immediately injected into onto a ZORBAX Eclipse XDB C8 column (2.1 mm × 15 mm, Agilent, Santa Clara, CA). Injected samples were desalted online for 3 min with 5% acetonitrile, 95% water, 0.1% formic acid, and eluted in 2 min using a gradient to 95% acetonitrile, 5% water, and 0.1% formic acid. The eluate was sent into a MaXis 4G Q-Tof mass spectrometer (Bruker) and mass spectra were deconvoluted using MagTran[16]. The mass of undeuterated protein was subtracted from the mass of the protein at each exchange-in time point and plotted. Each exchange point was analyzed with triplicates. No adjustment was made for deuterium back exchange during analysis because all interpretation required consideration of relative changes in HDX. Therefore, all results are reported as the relative deuterium level[17].

For peptide-level HDX analysis, following the quench and mixing, the protein mixture was immediately injected into a custom-built HDX device and passed through a column containing immobilized pepsin (2 mm × 20 mm) beads at a flow rate of 200 μL/min in 0.1% formic acid. The resulting peptic peptides were captured on a ZORBAX Eclipse XDB C8 column (2.1 mm × 15 mm, Agilent, Santa Clara, CA) for desalting (3 min). The flow through the C8 column was then switched in-line to a Hypersil Gold C18 column (2.1 mm × 50 mm, Thermo Fisher, Waltham, MA), and a linear gradient (4% to 40% acetonitrile, 0.1 % formic acid, 200 μL/min flow rate, over 5 min) was used to separate the peptides and direct

them in to a LTQ-FT mass spectrometer (Thermo Fisher, Waltham, MA) equipped with an electrospray ionization source. MS detection used the following instrument parameters: spray voltage 5 kV, capillary temperature 275 °C, capillary voltage 38 V, and tube lens 185 V. Data were collected at a mass resolving power of 100,000 at *m/z* 400. Each experiment was carried out in duplicate. The valves, columns, and tubing for desalting, protein digestion and HPLC separation were submerged in an ice-water bath to minimize back-exchange.

Peptide Identification and HDX Data Analysis

Peptide identification was accomplished through a combination of accurate mass analysis and LC-MSMS using Mascot (Matrix Science, London, UK), and the output peptide sets were manually checked and verified, as previously described[12]. Raw HDX spectra and peptide sets were submitted to HDX Workbench for calculation and data visualization in a fully automated fashion[18]. No EX-1 signature regarding to the exchange mechanism was observed. Deuterium uptake at each time point was calculated by subtracting the centroid of the isotopic distribution of the undeuterated peptide from that of the deuterated peptide, and the relative deuterium uptake was plotted versus the labeling time to afford HDX kinetic curves. For comparison between complex and control samples, differences in deuterium uptake level following all incubation time points were calculated and mapped onto the protein 3D structure for data visualization. All HDX data were normalized to 100% deuterium content, and no correction was made for back exchange because relative trends provided the needed information.

Results

Global HDX analyses

The HDX analysis of intact proteins can provide a relatively quick readout on the overall changes in solvent protection and hydrogen bonding that are induced by perturbations to a protein. Thus, we measured the HDX kinetics of intact DREAM in the absence and presence of Ca^{2+} to examine the global impact of Ca^{2+} binding to DREAM (Figure 1). To study the effects of Ca^{2+} binding on the intact DREAM quantitatively, we fit the kinetic curve with five rate constant bins (100, 10, 1, 0.1, and 0.01 min^{-1}) and the results were shown in Figure 1B. The full length DREAM contains 256 amino acid residues with 246 exchangeable backbone amide hydrogens (excluding 9 prolines and the N-terminal one). For the apo-DREAM, after 10 s of exchange, more than 120 backbone amide sites exchanged with deuterium, which is almost half of the total exchangeable amide hydrogens. The deuterium incorporation into protein leveled off rapidly after 20 min of exchange (Figure 1A). After curve fitting, 114 backbone amide sites were determined to have a fast exchange rate at 100 min^{-1}, which is in the range of the intrinsic exchange rate constant for unstructured residues. The properties of fast exchange for *apo*-DREAM suggest that large portion of the molecule is random-coiled and highly flexible in solution. In the presence of Ca^{2+}, the exchange was greatly reduced; only ~ 80 backbone amide sites exchanged with deuterium after 10 sec (Figure 1A). These changes induced by calcium binding clearly involve the shift of faster exchange residues (e.g., with rate constants in the range of 100 or 10 min^{-1}) to lower exchange ones (e.g., with rate constants of 0.1 or 0.01 min^{-1}). Moreover, calcium binding to DREAM results in 20 residues becoming non-exchangeable, reflected by the deuterium

uptake reaching a maximum of approximately 160 amides for Ca^{2+}-bound DREAM compared to 180 amides for *apo*-DREAM (Figure 1A).

Peptide-level HDX analysis of Apo WT DREAM

Because the rates of amide hydrogen exchange with solvent deuterium are determined by the local fluctuations in protein structure, HDX rates can be good readouts for protein conformational dynamics [19]. There is no published high resolution structure of *apo* DREAM available, and thus little is known about its conformation. To provide a coarse-grained structure and a measure of its dynamics, we first measured the HDX for the *apo* DREAM, especially for those functionally important EF-hands and the N-terminal region whose function is not highly settled. To form the basis of later comparisons with Ca^{2+} bound DREAM, we followed the HDX of *apo*-DREAM over the time course of 10 s to 4 h. The HDX kinetic curves for 105 DREAM peptic peptides covering ~95 % of the full length protein sequence are provided in Supplemental Figure S1. The average percentage of deuterium uptake of individual peptic peptides derived from *apo*-DREAM at each time point was mapped onto the NMR structure of Ca^{2+} and Mg^{2+} bound mouse DREAM (PDB:2JUL with metal ions removed to avoid confusion), as shown in Figure 2. The HDX data reveal that most of the N-terminal region (residues 7–79) is very flexible. Over 70% of amide hydrogens exchanged with deuterium within 10 s, and the extent of exchange becomes nearly constant for the remainder of the experiment. Interestingly, a peptide from the N-terminal region (residues 46–52), although flexible, maintained some protection, as exhibited by a slow uptake of deuterium with time. It is noteworthy that this region is defined as a leucine-charged residue rich domain (LCD) and is involved in protein-protein interactions between DREAM and other important transcription factors[20–22].

In the C-terminal Ca^{2+} binding region containing four EF-hand motifs, all the EF-hand loops (EF-1, residues 97–108; EF-2, residues 139–151; EF-3, residues 172–187; EF-4, residues 219–230) exhibit rapid HDX, showing a large uptake of deuterium even at the earliest exchange time, indicating high flexibility in structure. This property is likely reporting on the required plasticity of the EF hands needed to undergo large, rapid, and local structural changes to accommodate Ca^{2+} insertion and binding[23]. The peptides derived from the EF-hands helices covering 109–121 (α3), 130–135 (α4), 152–158 (α5), 160–173 (α6), and 188–198 (α7) incorporate deuterium nearly linearly during the time course of the experiment, indicating that these amide hydrogens are comparably protected, and the regions covered by the amides are clearly structured.

Overall, the structure of *apo*-DREAM is very flexible as revealed by maximum deuterium uptake of approximately half the protein within 10 s and over 90% exchange amide hydrogen reaches maximum deuterium uptake within 15 min at 4 °C. Taken together, our HDX data confirm *apo*-DREAM maintains a flexible and largely unstructured N-terminal and flank regions between the EF-hands, but the EF-hand helices are well structured.

Differential HDX analyses of WT DREAM/Ca^{2+} complex

The transcriptional activity of the repressor DREAM is mediated by the levels of nuclear calcium[1]. In a typical two-EF-hand domain, Ca^{2+}-induced conformation changes usually

involve the relative orientation of the helices flanking the Ca^{2+}-binding loops, thus causing a transition from a “closed” to an “open” domain conformation[24]. To understand Ca^{2+}-binding induced conformational changes of DREAM, we performed comprehensive differential HDX analysis of the full-length DREAM in the absence and presence of Ca^{2+}. Because we measured the HDX kinetics of peptic peptides derived from the *holo*-DREAM in an identical manner as for *apo*-DREAM, any changes in rates for individual peptides should reliably localize the Ca^{2+}-induced perturbations to the protein conformational dynamics (Kinetic plots comparing the HDX rates for all peptides between two states are displayed in Supplemental Figure S1). Upon Ca^{2+} binding, DREAM undergoes large conformational changes. As shown in Figure 3A, nearly the entire C-terminal Ca^{2+} binding regions exhibits dramatic protection from exchange following Ca^{2+} binding.

From the NMR structure (PDB: 2JUL)[7] and also from an early ITC study[25], we know that EF-2, EF-3 and EF-4 are Ca^{2+} binding sites. Consistent with these studies, the peptides covering these three entire EF hand regions showed massive protection from exchange (Figure 3A and B, Supplemental Figure S1). We can imagine that chelating Ca^{2+} by the side-chain oxygen atoms of EF2 (D139, D141, N143, D150), EF3 (D175, N177, D179, and E185), and EF4 (D223, N225, D227, E233) within the calcium-binding loop repositions the two helices within the EF-hands. In addition, the α-helices forming each EF-hands other than the calcium-binding loops also show pronounced protection from exchange (Figure 3A, Supplemental Figure S1), suggesting that the helices in *apo*-DREAM are less stable and the interactions between helices are more pronounced in *holo*-DREAM, consistent with the much less extensively hydrophobic packing of EF-hand helices for Calmodulin in the absence of Ca^{2+} observed by NMR[24].

Surprisingly, our HDX data illustrate that EF-1 also exhibited strong protection upon Ca^{2+} binding indicating large conformational changes in this EF-hand (Figure 3B). It should be recalled that EF-1 contains the CPXG sequence thought to prevent the interaction with Ca^{2+} by sterically disrupting the calcium binding loop’s structure, as was demonstrated for other NCS proteins [26, 27]. In addition, the NMR structure showed that the EF-1 loop in the N-terminal truncated DREAM is distorted from a favorable Ca^{2+}-binding geometry by the presence of Pro105 at the fourth position that places a kink in the middle of the loop[7]. More intriguingly, the deuterium incorporation to an N-terminal fragments of (residues 46–52) of Ca^{2+}-bound DREAM was markedly slowed by Ca^{2+} binding, but this region is remote from the EF hands (Figure 3C).

We also performed the differential HDX study at higher Ca^{2+} concentration, 5 mM. The protection from deuterium incorporation into EF-1 and 2 hands is robustly enhanced. As a comparison, there is detectable elevated protection for only EF-4 hand, but not for EF-3 (Figure 3B). These results suggest that Ca^{2+} binds to the EF-2 hand with lower affinity and to EF-3 with highest affinity. A previous ITC study of a series of single-site mutant constructs, which that disable functional Ca^{2+} binding to the individual EF-hands, shows that EF-2 hand has lower affinity site, and EF-3 and 4 are relatively higher affinity sites. That report also suggests that Ca^{2+} binds to EF-3 hand first, subsequently to EF-4 hand, and lastly to EF-hand 2. Accordingly, our HDX results show unsaturated Ca^{2+} binding to EF-2,

almost saturated binding to EF-4, and saturated binding to EF-3 at 100 uM Ca^{2+} (Figure 3B).

Interestingly, EF-1 hand, along with EF-2 hand, present enhanced protection at higher Ca^{2+} concentration, although EF-1 may not bind Ca^{2+}. This suggests that the full length DREAM may exhibit long range structural interactions between the EF-hands, facilitating cooperative structural changes.

Comparison of HDX of Ca^{2+}-bound WT DREAM and EF-1 mutants

The large conformational changes in EF-1 hand, as revealed by HDX, strongly suggest that EF-1 may also bind to Ca^{2+} in the context of the full-length protein. A μESI-mass spectrometry direct analysis of DREAM, however, suggests that four Ca^{2+} ions bind to full-length DREAM[5]. At first, it seemed that our HDX data are consistent with the μESI-mass spectrometry analysis of DREAM. To determine whether the first EF-hand binds to calcium, we made two mutant constructs (E111Q/D112N and E103A/D110A) by selectively substituting some critical Ca^{2+}-binding residues within EF-1 loop with the intention, to "abolish" as completely as possible its Ca^{2+} binding. We then conducted the same differential HDX experiments for these two mutant constructs in the absence and presence of Ca^{2+}. The HDX of EF-1 hand, as revealed by its peptic peptides in E111Q/D112N and E103A/D110A, should show minimal differences in the presence or absence of Ca^{2+} if there is no calcium binding in the mutant structures since this EF-hand loop cannot now be occupied. We found similar HDX protection in EF-hand 2, 3, and 4 for both DREAM mutants compared to the wild-type protein (Figure 4), indicating that the amino-acid substitutions in EF-1 did not affect Ca^{2+} binding to EF-hands 2, 3, and 4. Interestingly, both mutant constructs exhibit similar HDX protection in EF-1 as shown by the wild-type, suggesting that the conformation changes in EF-1 occurring for both the WT and mutants corresponds to a long-range or remote conformational change induced by Ca^{2+} binding to EF-hands 2, 3, and 4. The binding of four Ca^{2+} ions to the full length DREAM by the μESI-mass spectrometry is likely an artifact in gas phase.

Discussion

HDX-MS monitors the structural changes in solution with high spatial resolution between different states; such information is not readily available by other approaches involving solid state structures. Having such information is extremely important especially if structural changes are associated with protein function. Our HDX data have revealed allosteric interactions and remote conformational changes as a consequence of Ca^{2+} binding to EF 2, 3, and 4.

It is well documented that the EF-1 hand in DREAM, similar to other neuron calcium sensors (NCS), is distorted from a favorable Ca^{2+} binding topology and consequently it is not capable of binding to calcium [7]. HDX of DREAM shows EF-1 hand, like EF hands 2, 3, and 4, significant protection. These conformational changes still occur in the Ca^{2+}-binding deficient EF-1 hand mutant constructs, suggesting the conformational changes are induced by cooperative Ca^{2+}-binding to other EF-hands. EF-hand motifs in proteins[24] show that the two constituent helices are usually approximately antiparallel in the Ca^{2+}-free state. Ca^{2+}

binding induces an opening of two EF-hand helix fingers, resulting in almost perpendicular inter-helical angles. In fact, the interhelical angle for the EF-1 hand is 92 º, comparable to those of other Ca^{2+}-bound EF-hands[7]. Therefore, despite the absence of Ca^{2+} binding at EF1-hand in DREAM, this hand undergoes similar conformational changes as other EF-hands upon Ca^{2+}-binding, likely resulting from the extensive hydrophobic interaction of the residues from the first and last helices (helix B and helix E) of EF-hand pairs in the N-terminal domain[28].

Besides the protection of the non-bonding EF-1 hand, there is also unexpected protection in response to Ca^{2+} binding in the N-terminal region (residues 46–52), suggesting an allosteric conformational change. Furthermore, the HDX data suggest that Ca^{2+} binding occurs firstly to EF-3 and 4, and subsequently to EF-2. Thus, the Ca^{2+} binding conformational changes are transmitted from the C- to the N-terminus, thereby changing the conformation of the leucine-charged residue-rich domain found in the sequence CLVKWIL. The N-terminal region (residues 1–65) of DREAM is structurally unstable, so the structural changes revealed by HDX are not highly distinct [7]. There is some evidence that the N-terminal extension does not have a functional role, but it contains a leucine-charged domain at position 47, which does govern the interactions between DREAM and CREB[20, 21]. CREB is a cellular transcription factor, and it binds to certain DNA sequences called cyclic-AMP response elements (CRE), thereby regulating the transcription of the downstream genes. In the absence of Ca^{2+}, DREAM may bind via its leucine-charged residue-rich domain and the kinase-inducible domain of CREB. The interaction with DREAM blocks binding of CREB to CREB-binding protein and affects CRE-dependent transactivation. Furthermore, the interaction between DREAM and CREB is Ca^{2+}-dependent whereby Ca^{2+} binding abolishes DREAM's interaction with CREB. In addition, the transcription activity of CREB depends on its ability to recruit coactivator CBP[29, 30]. CBP binds to the kinase-inducible domain of CREB at the site for DREAM binding. As a result, the Ca^{2+}-dependent DREAM-CREB interaction modulates the ability of CREB to recruit CREB-binding protein and regulate the transactivation by the CREB-binding protein of CREB-dependent transcription. The Ca^{2+}-dependent DREAM-CREB interaction may require conformational changes that are communicated allosterically to the leucine-charged residue-rich domain of DREAM, and our HDX MS data provide evidence of this allosteric communication. It seems that the Ca^{2+} signal is transmitted to position 47 of the leucine-charged residue-rich domain of DREAM via the conformational changes from C-terminus to N-terminus. The conformational changes in LCD-47 upon Ca^{2+} binding could shield the critical residues involved in the interaction with CREB and make the interaction unfavorable.

Conclusion

Binding of Ca^{2+} to EF-hands in Ca^{2+}-binding proteins triggers conformational changes that underlie their Ca^{2+} dependent biological effects. Our HDX data provide considerable insight in the Ca^{2+} binding properties and the associated conformational changes, especially the long-range allosteric effects on the LCD in the N-terminal domain. This site was previously reported responsible for the interactions with CREM and CREB. Although our HDX data do not prove howCa^{2+} binding modulates DREAM binding to DNA, future studies can now characterize the structural interaction of DREAM bound to DRE genes at the molecular

level and map out the DNA binding region. Combined with the Ca^{2+} binding properties observed here, these studies should shed light on Ca^{2+} effects on gene expression.

Supplementary Material

Refer to Web version on PubMed Central for supplementary material.

Acknowledgments

This work was supported by the National Institutes of Health, NIGMS 8 P41 GM103422 to MLG

References

1. Carrion AM, Link WA, Ledo F, Mellstrom B, Naranjo JR. DREAM is a Ca2+-regulated transcriptional repressor. Nature. 1999; 398:80–84. [PubMed: 10078534]
2. Osawa M, Tong KI, Lilliehook C, Wasco W, Buxbaum JD, Cheng HYM, Penninger JM, Ikura M, Ames JB. Calcium-regulated DNA binding and oligomerization of the neuronal calcium-sensing protein, calsenilin/DREAM/KChIP3. Journal of Biological Chemistry. 2001; 276:41005–41013. [PubMed: 11535596]
3. Ledo F, Kremer L, Mellstrom B, Naranjo JR. Ca2+-dependent block of CREB-CBP transcription by repressor DREAM. Embo Journal. 2002; 21:4583–4592. [PubMed: 12198160]
4. Zhou Y, Frey TK, Yang JJ. Viral calciomics: interplays between Ca2+ and virus. Cell Calcium. 2009; 46:1–17. [PubMed: 19535138]
5. Craig TA, Benson LM, Venyaminov SY, Klimtchuk ES, Bajzer Z, Prendergast FG, Naylor S, Kumar R. The metal-binding properties of DREAM: evidence for calcium-mediated changes in DREAM structure. J Biol Chem. 2002; 277:10955–10966. [PubMed: 11788589]
6. Gifford JL, Walsh MP, Vogel HJ. Structures and metal-ion-binding properties of the Ca2+-binding helix-loop-helix EF-hand motifs. Biochemical Journal. 2007; 405:199–221. [PubMed: 17590154]
7. Lusin JD, Vanarotti M, Dace A, Li CM, Valiveti A, Ames JB. NMR structure of DREAM: Implications for Ca2+-dependent DNA binding and protein dimerization (vol 47, pg 2252, 2008). Biochemistry. 2008; 47:6088–6088.
8. Zhang Z, Smith DL. Determination of amide hydrogen exchange by mass spectrometry: a new tool for protein structure elucidation. Protein Sci. 1993; 2:522–531. [PubMed: 8390883]
9. Konermann L, Vahidi S, Sowole MA. Mass spectrometry methods for studying structure and dynamics of biological macromolecules. Anal Chem. 2014; 86:213–232. [PubMed: 24304427]
10. Zhang J, Chalmers MJ, Stayrook KR, Burris LL, Wang Y, Busby SA, Pascal BD, Garcia-Ordonez RD, Bruning JB, Istrate MA, Kojetin DJ, Dodge JA, Burris TP, Griffin PR. DNA binding alters coactivator interaction surfaces of the intact VDR-RXR complex. Nat Struct Mol Biol. 2011; 18:556–563. [PubMed: 21478866]
11. Iacob RE, Krystek SR, Huang RY, Wei H, Tao L, Lin Z, Morin PE, Doyle ML, Tymiak AA, Engen JR, Chen G. Hydrogen/deuterium exchange mass spectrometry applied to IL-23 interaction characteristics: potential impact for therapeutics. Expert Rev Proteomics. 2015; 12:159–169. [PubMed: 25711416]
12. Li J, Rodnin MV, Ladokhin AS, Gross ML. Hydrogen-deuterium exchange and mass spectrometry reveal the ph-dependent conformational changes of diphtheria toxin t domain. Biochemistry. 2014; 53:6849–6856. [PubMed: 25290210]
13. Wang H, Shu Q, Rempel DL, Frieden C, Gross ML. Continuous and Pulsed Hydrogen-Deuterium Exchange and Mass Spectrometry Characterize CsgE Oligomerization. Biochemistry. 2015; 54:6475–6481. [PubMed: 26418947]
14. Craig TA, Ramachandran PL, Bergen HR 3rd, Podratz JL, Windebank AJ, Kumar R. The regulation of apoptosis by the downstream regulatory element antagonist modulator/potassium channel interacting protein 3 (DREAM/KChIP3) through interactions with hexokinase I. Biochem Biophys Res Commun. 2013; 433:508–512. [PubMed: 23524266]

15. Ramachandran PL, Craig TA, Atanasova EA, Cui G, Owen BA, Bergen HR 3rd, Mer G, Kumar R. The potassium channel interacting protein 3 (DREAM/KChIP3) heterodimerizes with and regulates calmodulin function. J Biol Chem. 2012; 287:39439–39448. [PubMed: 23019329]
16. Zhang Z, Marshall AG. A universal algorithm for fast and automated charge state deconvolution of electrospray mass-to-charge ratio spectra. Journal of the American Society for Mass Spectrometry. 1998; 9:225–233. [PubMed: 9879360]
17. Wales TE, Engen JR. Hydrogen exchange mass spectrometry for the analysis of protein dynamics. Mass Spectrom Rev. 2006; 25:158–170. [PubMed: 16208684]
18. Pascal BD, Willis S, Lauer JL, Landgraf RR, West GM, Marciano D, Novick S, Goswami D, Chalmers MJ, Griffin PR. HDX workbench: software for the analysis of H/D exchange MS data. J Am Soc Mass Spectrom. 2012; 23:1512–1521. [PubMed: 22692830]
19. Krishna MM, Hoang L, Lin Y, Englander SW. Hydrogen exchange methods to study protein folding. Methods. 2004; 34:51–64. [PubMed: 15283915]
20. Ledo F, Carrion AM, Link WA, Mellstrom B, Naranjo JR. DREAM-alphaCREM interaction via leucine-charged domains derepresses downstream regulatory element-dependent transcription. Mol Cell Biol. 2000; 20:9120–9126. [PubMed: 11094064]
21. Ledo F, Kremer L, Mellstrom B, Naranjo JR. Ca2+-dependent block of CREB-CBP transcription by repressor DREAM. EMBO J. 2002; 21:4583–4592. [PubMed: 12198160]
22. Scsucova S, Palacios D, Savignac M, Mellstrom B, Naranjo JR, Aranda A. The repressor DREAM acts as a transcriptional activator on Vitamin D and retinoic acid response elements. Nucleic Acids Res. 2005; 33:2269–2279. [PubMed: 15849313]
23. Zhang J, Chalmers MJ, Stayrook KR, Burris LL, Garcia-Ordonez RD, Pascal BD, Burris TP, Dodge JA, Griffin PR. Hydrogen/Deuterium Exchange Reveals Distinct Agonist/Partial Agonist Receptor Dynamics within Vitamin D Receptor/Retinoid X Receptor Heterodimer. Structure. 2010; 18:1332–1341. [PubMed: 20947021]
24. Zhang M, Tanaka T, Ikura M. Calcium-induced conformational transition revealed by the solution structure of apo calmodulin. Nat Struct Biol. 1995; 2:758–767. [PubMed: 7552747]
25. Osawa M, Dace A, Tong KI, Valiveti A, Ikura M, Ames JB. Mg2+ and Ca2+ differentially regulate DNA binding and dimerization of DREAM. J Biol Chem. 2005; 280:18008–18014. [PubMed: 15746104]
26. Flaherty KM, Zozulya S, Stryer L, McKay DB. Three-dimensional structure of recoverin, a calcium sensor in vision. Cell. 1993; 75:709–716. [PubMed: 8242744]
27. Ames JB, Tanaka T, Stryer L, Ikura M. Portrait of a myristoyl switch protein. Curr Opin Struct Biol. 1996; 6:432–438. [PubMed: 8794166]
28. Vijay-Kumar S, Kumar VD. Crystal structure of recombinant bovine neurocalcin. Nat Struct Biol. 1999; 6:80–88. [PubMed: 9886296]
29. Chrivia JC, Kwok RP, Lamb N, Hagiwara M, Montminy MR, Goodman RH. Phosphorylated CREB binds specifically to the nuclear protein CBP. Nature. 1993; 365:855–859. [PubMed: 8413673]
30. Kwok RP, Lundblad JR, Chrivia JC, Richards JP, Bachinger HP, Brennan RG, Roberts SG, Green MR, Goodman RH. Nuclear protein CBP is a coactivator for the transcription factor CREB. Nature. 1994; 370:223–226. [PubMed: 7913207]

(A)

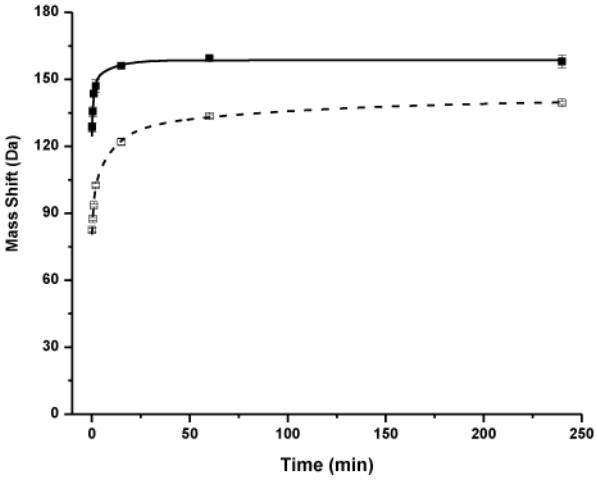

(B)

Sample	Total amides	No. of amide hydrogens at each fixed rate (k /min^{-1}) bin					
		100	10	1	0.1	0.01	Non exchangeable
Apo	246	114	14	21	10	0	86
Holo	246	78	0	21	27	14	106

Figure 1.

HDX analyses of intact DREAM. (A) The intact DREAM HDX was analyzed at seven different time points in triplicate. The solid (■) and open squares (□) represent the deuterium uptake levels at exchange time for *apo*-DREAM and *holo*-DREAM, respectively. The intact HDX data were fit (solid line for apo-DREAM and dashed line for holo-DREAM) with first order exponential model with five fixed rate-constant bins (k = 100, 10, 1, 0.1, and 0.01 min^{-1}) using Prism. (B) The kinetic modeling "binned" the number of amides with respect to five fixed rate constants.

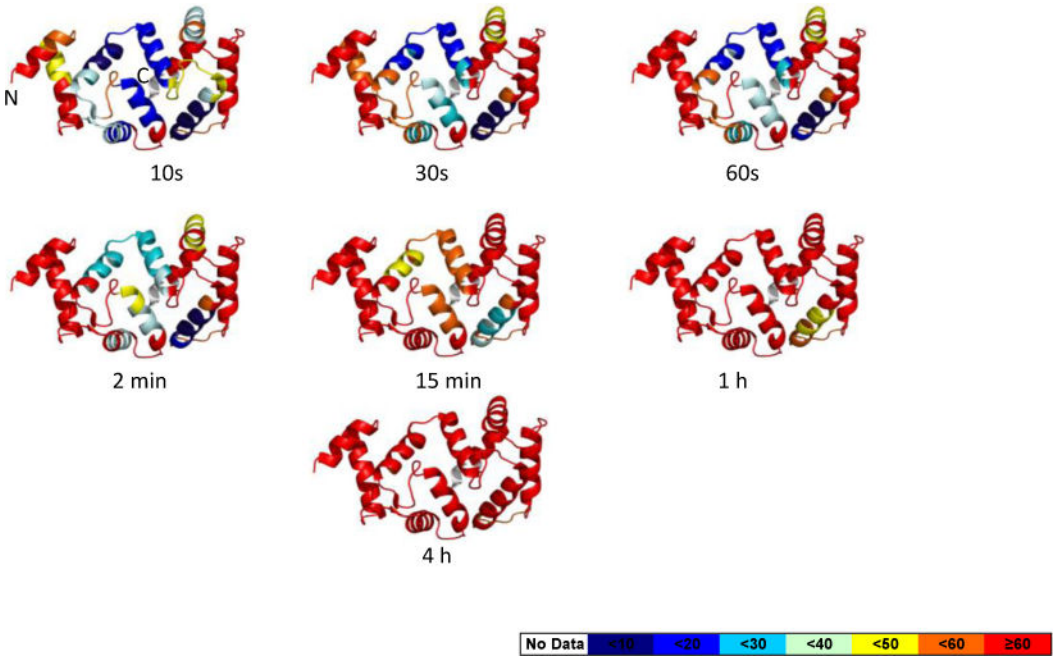

Figure 2.

HDX dynamics of *apo*-DREAM is mapped onto the 3D structures of *holo* DREAM (PDB: 2JUL with metal ions removed to avoid confusion) with color for each exchange time at 10 s, 30 s, 1 min, 2 min, 15 min, 1 h and 4 h of exposure in D_2O buffer. The color code indicates the percentage of deuterium update, as explained at the bottom of the figure. Peptides representing regions colored as white were not detected.

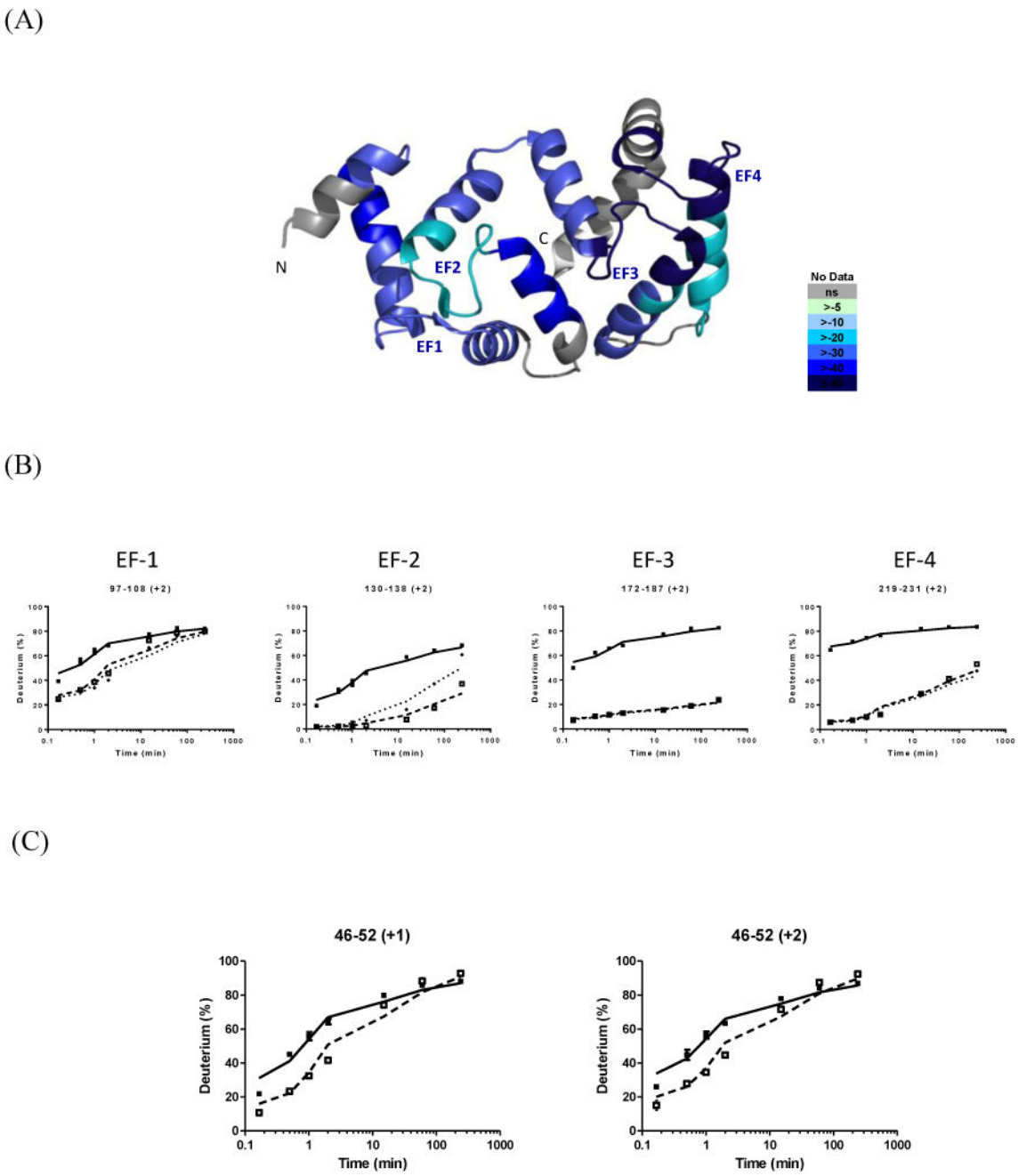

Figure 3.

(A) Average percentage differences in deuterium uptake between *apo* and *holo* states of wild type DREAM mapped onto the NMR structure (2JUL) of *holo* DREAM. The residue numbers for four EF-hand are: EF-1, residues 90–119; EF-2, residues 128–157; EF-3, residues 163–192; and EF-4, residues 211–240 (the sequences are in Table 1). (B) Deuterium uptake plots of selected peptides derived from the representative region of each EF-hand of DREAM at different Ca^{2+} concentrations. Solid lines represent the deuterium incorporation of the peptides from DREAM in the absence of Ca^{2+}; the dashed lines represent the deuterium incorporation of the peptides from DREAM incubated in 100 uM

Ca^{2+}; the dotted line represent the deuterium incorporation of the peptide from DREAM incubated in 5 mM Ca^{2+}. (C) Deuterium uptake plots of the peptide (CLVKWIL) from the N-terminal region containing the LCD.

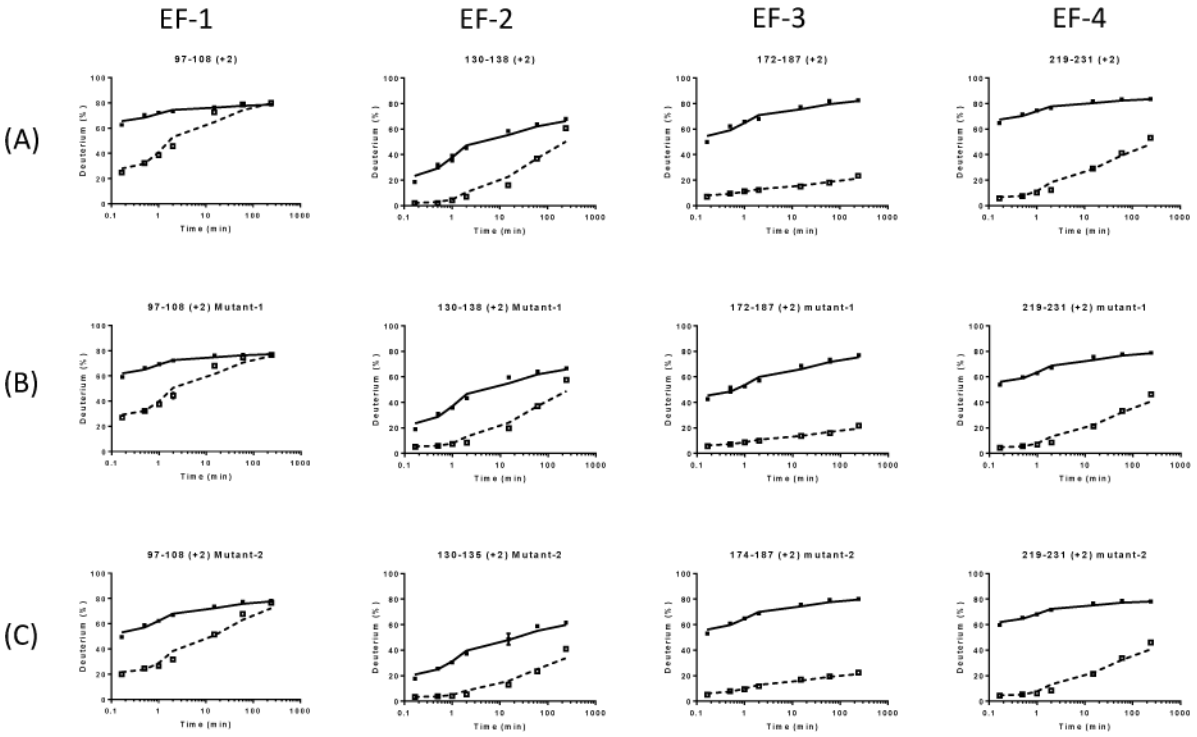

Figure 4.

Comparison of Ca^{2+} binding induced conformational changes in EF-hands for (A) wild-type DREAM, (B) EF-1 mutant E111Q/D112N, and (C) E103A/D110A. The relative percentage of deuterium incorporation was shown for representative peptides from each EF-hand. Solid lines represent the deuterium incorporation of the peptides from DREAM in the absence of Ca^{2+}; the dashed lines represent the deuterium incorporation of the peptides from DREAM incubated in the presence of Ca^{2+}.

Table 1

The four EF Hands of DREAM. The blue columns represent the residues whose side chains serve as ligands for Ca^{2+}. Residue 6 is a conserved Gly, as usual, and 8 is hydrophobic. X, Y, and Z represent the usual binding sites.

EF	X 1	2	Y 3	4	Z 5	6	−Y 7	8	−X 9	10	11	−Z 12
1	N	E	C	P	T	G	L	V	D	E	D	
2	D	A	D	G	N	G	A	I	H	F	E	D
3	D	I	N	K	D	G	Y	V	T	K	E	E
4	D	R	N	Q	D	G	V	V	T	I	E	E